

# Driving-induced many-body localization

Eyal Bairey,<sup>1</sup> Gil Refael,<sup>2</sup> and Netanel H. Lindner<sup>1</sup>

<sup>1</sup>*Physics Department, Technion, 3200003, Haifa, Israel*

<sup>2</sup>*Institute for Quantum Information and Matter, Caltech, Pasadena, CA 91125, USA*

Subjecting a many-body localized system to a time-periodic drive generically leads to delocalization and a transition to ergodic behavior if the drive is sufficiently strong or of sufficiently low frequency. Here we show that a specific drive can have an opposite effect, taking a static delocalized system into the MBL phase. We demonstrate this effect using a one dimensional system of interacting hardcore bosons subject to an oscillating linear potential. The system is weakly disordered, and is ergodic absent the driving. The time-periodic linear potential leads to a suppression of the effective static hopping amplitude, increasing the relative strengths of disorder and interactions. Using numerical simulations, we find a transition into the MBL phase above a critical driving frequency and in a range of driving amplitudes. Our findings highlight the potential of driving schemes exploiting the coherent suppression of tunneling for engineering long-lived Floquet phases.

A key obstacle in the search for new non-equilibrium quantum phases of matter is the tendency of closed quantum many-body systems to indefinitely absorb energy from a time-periodic driving field. Thus, in the long time limit, such systems generically reach a featureless infinite-temperature-like state with no memory of their initial conditions [1–8]. Interestingly, this infinite temperature fate can be avoided by addition of disorder [9–13]. Sufficiently strong disorder added to a clean interacting system may lead to a many-body localized (MBL) phase [14–18] which does not allow transport of energy and particles. The MBL phase can persist in the presence of a weak high-frequency drive [9–13]. Periodically driven systems in the MBL phase retain memory of their initial conditions for arbitrarily long times. Thus, they can support non-equilibrium quantum phases of matter, including some which are unique to the non-equilibrium setting [19–30].

Generically, subjecting an MBL system to a periodic drive increases the localization length [9–11]. If the driving is done at sufficiently low frequencies or high amplitudes, it may even cause the system to exit the MBL phase. This delocalization effect is caused by transitions such as photon-assisted hopping, which are mediated by the periodic drive. These transitions conserve energy only modulo  $\hbar\omega$ , and can therefore lead to new many-body resonances which destabilize localization.

An oscillating linear potential (henceforth an AC electric field) has a more subtle effect, as it can effectively suppress the hopping amplitude between adjacent lattice sites. This effect, called dynamical localization [33] or coherent destruction of tunneling [34], has been implemented in cold atoms [35, 36], and can be used for example to induce a transition from a Bose-Einstein condensate to a Mott insulator in the Bose-Hubbard model [37, 38]. In non-interacting systems, dynamical localization can also be employed to tune the localization properties of one dimensional disordered lattices [39–42]. In an interacting disordered system, we expect the suppression of the hopping amplitude to increase the relative

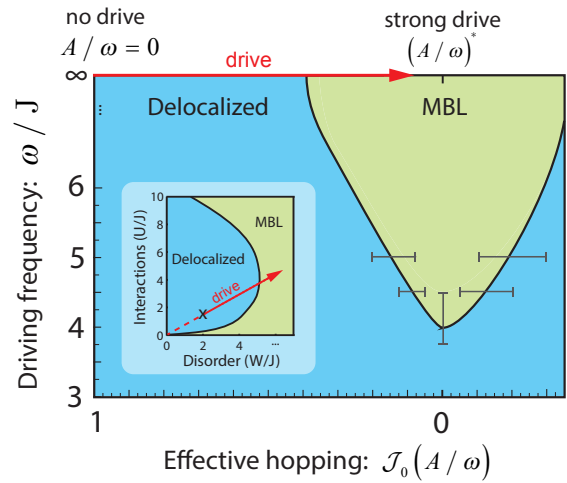


Figure 1. Phase diagram showing the MBL phase induced by time-periodic driving. Hardcore bosons with nearest-neighbor interactions on a weakly disordered 1D lattice enter an MBL phase when driven by an AC electric field above a critical driving frequency and in a range of driving amplitudes. The horizontal axis corresponds to the effective hopping amplitude  $J_{eff}/J = J_0(A/\omega)$  where  $J_0$  is the zeroth Bessel function, and  $A$  is the AC field’s amplitude. Only values of  $A/\omega \geq 0$  up to the first minimum of  $J_0$  are shown. The vertical axis corresponds to the driving frequency. The phase boundaries are extracted from finite size scaling of quasi-energy level statistics (see Figs. 2,4,5 and Appendix B). Inset: schematic undriven phase diagram as a function of disorder  $W/J$  and interaction  $U/J$  strength, as numerically obtained by [31, 32]. The cross marks the parameters chosen for our simulations; the red arrow indicates the effective change of parameters due to the suppression of  $J_{eff}$  by the periodic drive.

strengths of disorder and interactions, potentially driving a static delocalized system towards the MBL phase (Fig. 1, inset). It is unclear though to what extent the phenomenon of dynamical localization, obtained to lowest order in inverse frequency expansions, still applies in interacting systems, where these expansions often di-

verge in the thermodynamic limit at any finite driving frequency [7, 43, 44].

Here we demonstrate that an AC electric field effects disordered many-body systems very differently than generic, time-periodic drives. In fact, we show that an ergodic (delocalized) system subjected to an AC electric field may transition into the MBL phase. Our results are summarized in Fig. 1, displaying the phase diagram of a one dimensional many-body system which would be ergodic in the absence of driving. Our main finding is a driving-induced MBL phase emerging in a range of driving amplitudes above a critical frequency  $\omega_c$ .

### Model

We consider interacting hardcore bosons hopping on a disordered one dimensional lattice with periodic boundary conditions at half filling  $N = L/2$ . The particles can hop to neighboring sites with a hopping amplitude  $J$ ; they interact with nearest-neighbor repulsion  $U$ , and are subject to random on-site potentials  $V_i$  drawn uniformly and independently from the interval  $[-W, W]$ . The static Hamiltonian in the absence of driving therefore takes the form:

$$H_{stat}(J, U, W) = J \sum_i \left( \hat{c}_{i+1}^\dagger \hat{c}_i + h.c. \right) + \sum_i V_i \hat{n}_i + U \sum_i \hat{n}_i \hat{n}_{i+1} \quad (1)$$

Variants of this model have been studied extensively [17, 31, 32, 45], and feature a transition to a many-body localized phase for sufficiently strong disorder. Specifically, starting from any point on the phase diagram in normalized disorder  $W/J$  and interactions  $U/J$  and decreasing the hopping amplitude  $J$  leads inevitably to the MBL phase (Fig. 1).

We investigate the effect of adding an AC electric field to this static model. We work in a gauge where the AC electric field is induced by a temporally oscillating, spatially uniform vector potential, rather than by a scalar potential. Using periodic boundary conditions, our system is thus equivalent to a ring penetrated by an oscillating magnetic flux. Parameterizing the electric field as  $E(t) = A \cos(\omega t)$ , the Peierls substitution [46] yields a complex phase for the hopping amplitude replacing  $\hat{c}_{i+1}^\dagger \hat{c}_i$  in Eq. (1) with  $\hat{c}_{i+1}^\dagger \hat{c}_i e^{-i \frac{A}{\omega} \sin(\omega t)}$  [37].

Intuitively, the AC field can lead to destructive interference of hopping amplitudes between neighboring sites, thus effectively suppressing the hopping amplitude  $J$ . This effect can be directly seen by considering the time-averaged Hamiltonian  $H_{eff} = \int_0^T H_{driven}(t) dt$ . While the disorder and interaction terms are unchanged by this averaging, time-averaging the oscillating phase yields

a renormalized effective hopping amplitude  $J_{eff}/J = \mathcal{J}_0(A/\omega)$ , where  $\mathcal{J}_0$  is the zeroth Bessel function. Therefore,  $H_{eff} = H_{stat}(J_{eff}, U, W)$ . When  $J_{eff}$  is larger than the critical value for localization  $J_c$  in the undriven model  $H_{stat}$ , the time-averaged Hamiltonian  $H_{eff}$  is delocalized. Thus, writing  $H(t) = H_{eff} + \sum_n \mathcal{J}_n(A/\omega) \hat{c}_{i+1}^\dagger \hat{c}_i e^{-i \omega n t} + h.c.$  (where  $\mathcal{J}_n$  are the Bessel functions of order  $n$ ), we expect the driven system to remain in the delocalized phase for  $J_{eff} > J_c$ .

For  $J_{eff} < J_c$ , the time-averaged Hamiltonian  $H_{eff}$  enters the MBL phase, and we expect the system to become localized above a critical frequency  $\omega > \omega_c$  [9–11, 47]. The drive consists of a sum of local operators. Eigenstates of  $H_{eff}$  coupled by such a local operator can only differ by the values of local integrals of motion within a range  $\xi$  of the operator's support [48–51], where  $\xi$  is of the order of the localization length. Absorption of energy from the drive is therefore expected to be suppressed if the driving frequency is larger than the typical local spectrum of a subsystem of size  $\xi$  [9]. Consequently, the lower critical frequency for inducing localization  $\omega_c$  should be minimal at  $J_{eff} = 0$ , when  $H_{eff}$  is trivially localized with  $\xi = 1$  and its local integrals of motion are simply the particle occupations  $n_i$ . When  $J_{eff}$  is increased,  $H_{eff}$  should become more weakly localized with a larger localization length  $\xi$  and correspondingly a larger local spectrum. We therefore expect the critical frequency to increase with  $J_{eff}$ , until it diverges at  $J_{eff} = J_c$  where  $H_{eff}$  delocalizes.

### Results

We tune the parameters of our static Hamiltonian to the delocalized phase:  $U = 1.5J$ ,  $W = 2J$ , and test whether it is localized for various driving frequencies and amplitudes. Specifically, we examine the quasi-energy level statistics of the evolution operator  $U(T)$  (up to a system size  $L = 16$ ), and the relaxation in time of an initially prepared product state (up to  $L = 20$ ). We first establish localization for strong driving at high frequencies, and then look at the effect of lower frequencies.

*Finite size scaling of quasi-energy level statistics.* We compute the evolution operator over one driving period  $U(T)$  by exponentiating  $H(t)$  at discrete time-steps (120 equally spaced steps) using exact diagonalization (ED). We then diagonalize  $U(T)$  to obtain the quasi-energies  $\epsilon_\alpha$ , and focus on the gaps between subsequent quasi-energies  $\delta_\alpha = \epsilon_{\alpha+1} - \epsilon_\alpha$ . The ratio between subsequent gaps averaged over the quasi-energy spectrum  $\langle r \rangle = \frac{\min(\delta_\alpha, \delta_{\alpha+1})}{\max(\delta_\alpha, \delta_{\alpha+1})}$  measures the energy level repulsion, and distinguishes between the MBL and delocalized phases [10, 17, 43]. The MBL phase is integrable and features uncorrelated Poisson level statistics with a level spacings parameter  $\langle r \rangle_{POI} \approx 0.39$ . The delocal-

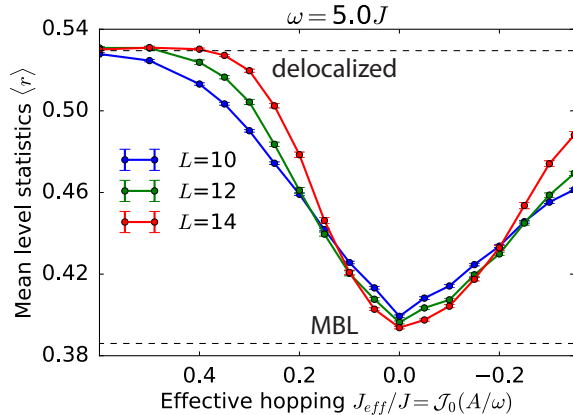


Figure 2. Finite-size scaling of quasi-energy level statistics as a function of driving amplitude at high driving frequency ( $\omega = 5J$ ). At weak driving the average level statistics parameter  $\langle r \rangle$  increases with system size and approaches the Wigner-Dyson value  $\langle r \rangle \approx 0.53$  corresponding to the delocalized phase. As the driving amplitude increases and the effective hopping is more strongly suppressed, this trend is reversed: the level statistics parameter decreases with system size, approaching the Poisson value  $\langle r \rangle \approx 0.39$  (lower dashed line) which corresponds to the localized phase. Further increase of driving amplitude leads to a revival of the effective hopping with an opposite sign, restoring the delocalized phase (only values of  $A/\omega \geq 0$  up to the first minimum of  $J_0$  are shown). Error bars indicate one standard deviation of the average, with averaging performed over at least 1000, 200, 100 disorder realizations for  $L = 10, 12, 14$  respectively.

ized phase is ergodic and features Wigner-Dyson statistics with energy level repulsion and therefore a larger value  $\langle r \rangle_{COE} \approx 0.53$  corresponding to the circular orthogonal ensemble (COE) of random matrices.

We begin by considering a fixed frequency  $\omega = 5J$  and increasing driving amplitudes, see Fig. 2. We observe a sharp change in the scaling of the level statistics with the system size as we increase the driving amplitude. When the system is weakly driven, the level statistics parameter becomes larger as the system size is increased, approaching the delocalized value  $\langle r \rangle_{COE} \approx 0.53$  similarly to the undriven case [31]. However, at sufficiently strong driving the effective hopping  $J_{eff}/J = J_0(A/\omega)$  is suppressed, and this trend is reversed: the level statistics parameter rather decreases as the system size is increased, approaching the MBL value  $\langle r \rangle_{POI} \approx 0.39$ . Thus, the drive induces a transition from the delocalized phase into the MBL phase. At even stronger driving amplitude the  $J_{eff}$  rises again (with an opposite sign), and the delocalized phase is recovered. We estimate the critical  $J_{eff}$  for this phase transition (marked in Fig. 1) according to finite-size scaling at the crossing of the curves for different system sizes  $L$  (see Appendix B).

The system sizes we study might exhibit finite size ef-

fects, since the width of their many-body spectrum is comparable to the driving frequency. Computation of the full evolution operator  $U(T)$  is expensive in time and memory, and even for  $L = 14$  the bulk of the energy levels are within a range of  $\approx 7J$  (measured by twice the standard deviation of the undriven energy spectrum), rendering resonant absorption of energy from the drive less prominent than in the thermodynamic limit. To confirm the existence of the localized phase at strong driving, we study larger systems by propagating an initial density pattern in time.

*Relaxation of an initial product state.* We initialize our system in an arbitrary product state at half filling, distributing  $L/2$  particles randomly among its  $L$  sites while keeping the rest of the sites empty. We then evolve this state for a long time by acting on it with the exponential of the Hamiltonian at discrete time steps (120 steps per period for over 1500 driving periods), and follow the site occupations  $\langle \hat{n}_i(t) \rangle$ . In the absence of driving, the particles spread throughout the system, such that the occupancy in each site eventually revolves around  $\langle \hat{n}_i \rangle \approx 0.5$  (Fig. 3a, bottom), corresponding to a thermal state.

As expected from the ED results, when we now evolve the same state with a strong drive at high frequency ( $\omega = 5J$ ), the particles remain mainly in their initial positions for the duration of our simulation, indicating long-term memory of the initial conditions, a signature of the MBL phase (Fig. 3a, top). Following [13, 52–54], we differentiate between the two phases by tracking the evolution of the generalized imbalance (also known as temporal autocorrelation [55] and Edwards-Anderson order parameter [56]), which measures the correlation between the current and initial density patterns,

$$\mathcal{I}(t) = \frac{4}{L} \sum_{i=1}^L \langle \psi(0) | \left( \hat{n}_i(t) - \frac{1}{2} \right) \left( \hat{n}_i(0) - \frac{1}{2} \right) | \psi(0) \rangle. \quad (2)$$

The imbalance generalizes a technique used in recent cold atom experiments, which studied the relaxation of an initially prepared charge-density-wave [52, 53].

In the absence of driving, the system is ergodic, and the density pattern becomes uncorrelated with the initial pattern. Thus, the imbalance decays to a value which decreases with system size (Fig. 3b, c). When the drive is applied, memory of the initial occupancy pattern persists for long times, and the imbalance stabilizes on a finite value independent on the system size ( $\mathcal{I} \approx 0.6$  for  $\omega = 5J$ ,  $J_{eff} = 0$ ). Thus, in the strong driving regime the system fails to thermalize, indicating that an MBL phase is induced by the driving field.

*Lower critical frequency:* Tuning the driving amplitude to optimal suppression of hopping ( $J_{eff} = 0$ ) and repeating the level statistics analysis for varying frequencies, we find a minimal critical frequency for inducing localization with the driving field we considered. For our

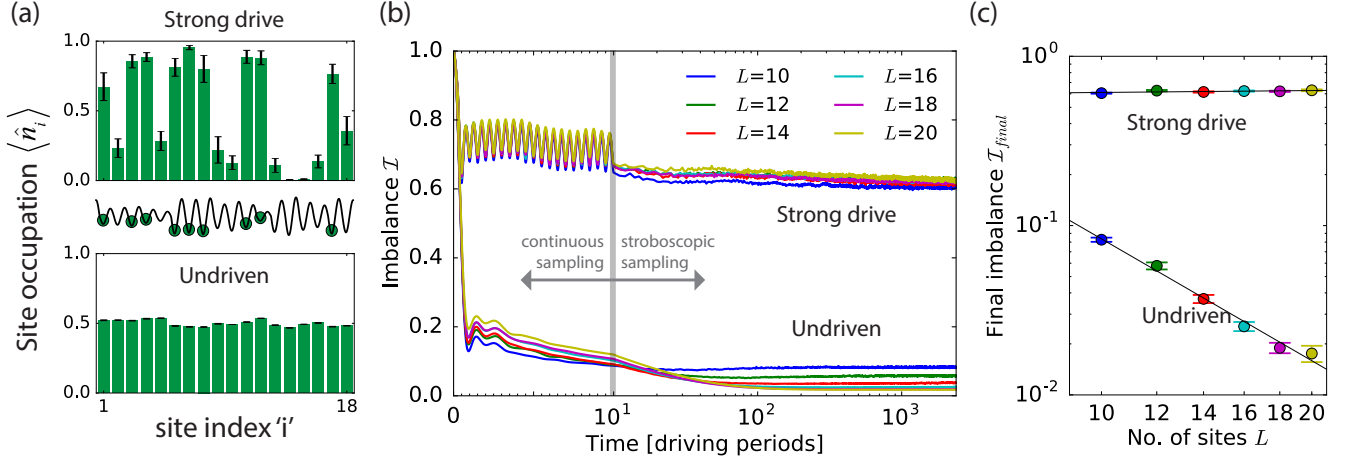


Figure 3. Relaxation of the occupation imbalance starting from a product state. (a) Example of site occupations  $\langle n_i \rangle$  at long times with a strong high-frequency drive (top;  $\omega = 5J$ ,  $J_{eff} = 0$ ) vs. an undriven system (bottom) starting from the same initial product state (middle). The occupations are averaged over  $10^3T < t < 1.5 \times 10^3T$  with error bars indicating one standard deviation accounting for fluctuations in that duration. (b) Imbalance [see Eq. (2)] as a function of time with (top) vs. without (bottom) a strong high-frequency drive ( $\omega = 5J$ ,  $J_{eff} = 0$ ), averaged over disorder realizations and random initial product states (1000 instances for  $L = 10$ , 500 for  $12 \leq L \leq 18$  and 200 for  $L = 20$ ). The imbalance is measured at each simulation step and shown on a linear time scale up to  $t = 10T$ , after which it is measured at stroboscopic times  $t = nT$  only and shown on a logarithmic time scale. While in the absence of driving site occupations become uncorrelated with their initial values, in the driven case they remain highly correlated. (c) Final imbalance as a function of system size (log-log scale), averaged over  $1.4 \times 10^3T < t < 1.5 \times 10^3T$ ; error bars indicate one standard deviation of the average over disorder realizations. The final imbalance decreases with system size in the absence of driving (slope =  $-2.4 \pm 0.2$ ), whereas it is insensitive to system size when the drive is applied (slope =  $0.04 \pm 0.03$ ).

choice of model parameters, our numerical results indicate that this critical frequency is  $\omega_c \approx 4J$ . As shown in Fig. 4, below this frequency, the level statistics pa-

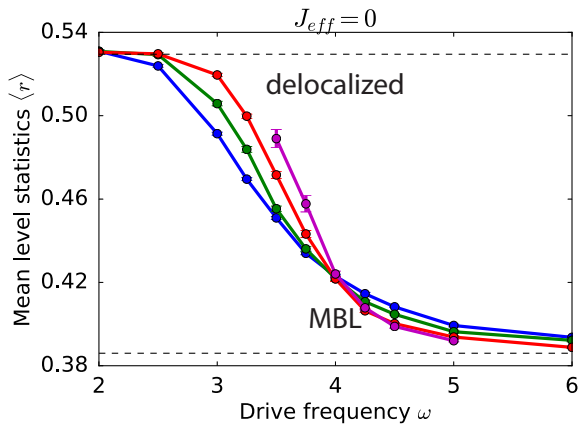


Figure 4. Quasi-energy level statistics  $\langle r \rangle$  as a function of driving frequency for  $J_{eff}(A/\omega) = 0$ . The changing trend in the scaling of  $\langle r \rangle$  with system size indicates a critical frequency  $\omega_c$  ( $\approx 4J$  for our parameters) above which driving-induced localization occurs.

rameter  $\langle r \rangle$  tends to its delocalized value as the system size increases. Indeed, if we now fix the driving frequency slightly below the critical frequency (specifically, we took  $\omega = 3.5J$ ) and apply a drive at increasing amplitudes, the level statistics parameter  $\langle r \rangle$  increases with system size for all driving amplitudes (Fig. 5b,c in Appendix A). Furthermore, evolving random product states at  $\omega = 3.5J$  and optimal suppression of hopping ( $J_{eff} = 0$ ), the generalized imbalance now decays slowly to a value which decreases with increasing system size (Fig. 6 in Appendix A). As expected, the lower critical frequency for inducing the MBL in our system increases with increasing  $J_{eff}$ , as can be seen from the phase diagram in Fig. 1.

## Discussion

We have shown that subjecting an ergodic system to a periodic drive can induce a transition into the MBL phase, providing an interesting example for the emergence of integrability in an ergodic system due to the addition of a drive. It would be interesting to understand how the phase diagram (Fig. 1) depends on the strength of disorder and interactions, and specifically, whether MBL can be induced in our model starting from arbitrarily weak disorder. Especially interesting are pos-

sible generalizations to higher dimensions, for example by using circularly polarized electromagnetic fields in two dimensions [57]. Most importantly, our results open new possibilities for inducing exotic out-of equilibrium phases in weakly disordered systems using methods which are readily accessible in cold atom systems [35, 36, 53].

### Acknowledgments

We thank Dima Abanin, Jens Bardarson, Iliya Esin, Vladimir Kalnizky, Ilia Khait, Roderich Moessner and Alon Nahshony for illuminating discussions. E. B. acknowledges financial support from the Gutwirth foundation. G. R. is grateful for support from the NSF through Grant No. DMR-1410435, the Institute of Quantum Information and Matter, an NSF Frontier center funded by the Gordon and Betty Moore Foundation, and the Packard Foundation. N. L. acknowledges support from the People Programme (Marie Curie Actions) of the European Union's Seventh Framework Programme (No. FP7/2007–2013) under REA Grant Agreement No. 631696, from the Israeli Center of Research Excellence (I-CORE) “Circle of Light.”, and from the European Research Council (ERC) under the European Union Horizon 2020 Research and Innovation Programme (Grant Agreement No. 639172).

*Note added:* During the completion of this manuscript, we became aware of a recent work [58] which finds localization enhancement in the driven quantum random energy model.

### Appendix A: closer look at lower driving frequencies

At  $\omega = 5J$  we found driving-induced many-body localization in a range of driving amplitudes around  $J_{eff} = 0$  (Fig. 2). We expect this range to vanish for  $\omega < \omega_c \approx 4J$  when the drive fails to induce localization even at  $J_{eff} = 0$  (Fig. 4). Indeed, when we perform finite size scaling of the level statistics as a function of driving amplitude at frequencies lower than  $5J$ , we find that the range of localization-inducing driving amplitudes continuously narrows, and all but shrinks to a point  $J_{eff} = 0$  at  $\omega = 4J$  (Fig. 5a, b). Below this frequency, the level statistics parameter increases with system size for any driving amplitude we tested, indicating that the drive fails to induce localization.

The lack of localization at low driving frequencies is also manifested in the relaxation of initial product states of particle occupations. When these states are driven at  $\omega = 3.5J$ , their generalized imbalance decays to a value which decreases with system size (Fig. 6), as in the undriven case. Note that the decay as a function of time is slower when compared to the decay in the undriven case. Presumably, this is due to the proximity

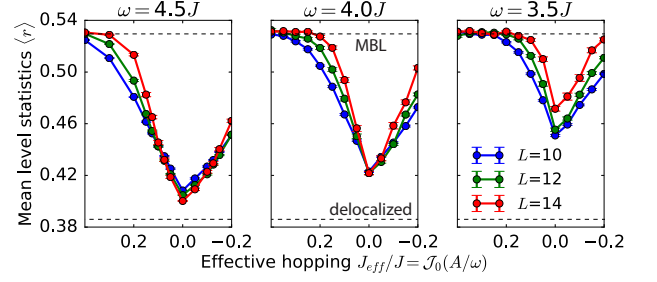


Figure 5. Quasi-energy level statistics as a function of driving amplitude at different driving frequencies. When the driving frequency is lowered, the range of driving amplitudes which induce many body localization narrows around  $(A/\omega)^*$  corresponding to the optimal suppression of hopping amplitude  $J_{eff} = 0$ . At  $\omega = 4J$ , the level statistics parameter changes very slowly with system size, indicating proximity to the critical frequency; at a lower frequency  $\omega = 3.5J$ , the level statistics parameter tends to the delocalized value at any driving amplitude we simulated.

to the MBL transition [54] for this value of the driving frequency. As the driving frequency approaches the speculated critical frequency  $\omega_c \approx 4J$ , the remaining imbalance at long times declines much slower with system size (Fig. 6 inset). The quick flattening of the slope in the inset of Fig 6, for a small change of driving frequency, provides an independent corroboration for the value of the critical frequency.

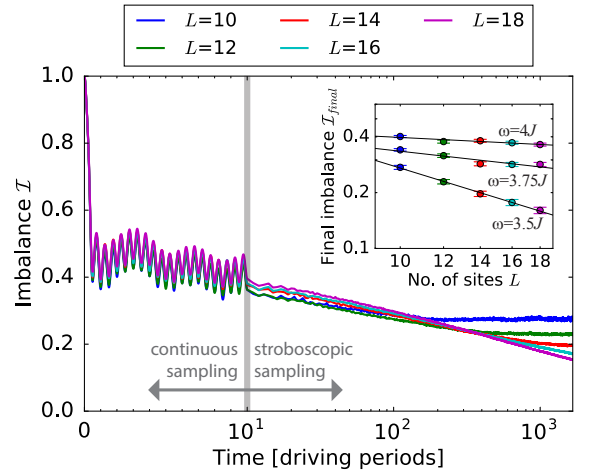


Figure 6. Imbalance as a function of time for optimal suppression of hopping  $J_{eff} = 0$  at low driving frequency  $\omega = 3.5J$ . At long times the imbalance decays with system size, indicating that the system is in the delocalized phase as expected from level statistics analysis. Inset: final imbalance (averaged over  $1.4 \times 10^3 T < t < 1.5 \times 10^3 T$ ) as a function of system size for different frequencies. The values for the slopes are  $-0.91 \pm 0.04$ ,  $-0.33 \pm 0.12$ ,  $-0.15 \pm 0.06$  for  $\omega = 3.5J$ ,  $3.75J$ ,  $4J$  respectively. The vanishing slope indicates a transition close to  $\omega_c \approx 4J$ .

## Appendix B: phase boundaries between the ergodic and MBL phases

The phase boundaries in Fig. 1 were obtained by finite size scaling of the data shown in Figs. 2, 4-5. Namely, a consistent increase of level statistics with system size is interpreted as an indication for the ergodic phase, while a consistent decrease of level statistics with system size is interpreted as an indication for the MBL phase. Error bars indicate parameter ranges where the trend in level statistics with increasing system size is inconsistent or not statistically significant (according to the error bars in Figs. 2, 4-5).

- 
- [1] L. D'Alessio and M. Rigol, *Physical Review X* **4**, 041048 (2014).
  - [2] A. Lazarides, A. Das, and R. Moessner, *Physical Review E* **90**, 012110 (2014).
  - [3] A. Lazarides, A. Das, and R. Moessner, *Phys. Rev. Lett.* **112**, 150401 (2014).
  - [4] A. Chandran and S. L. Sondhi, *Physical Review B* **93**, 174305 (2016).
  - [5] R. Citro, E. G. Dalla Torre, L. D'Alessio, A. Polkovnikov, M. Babadi, T. Oka, and E. Demler, *Annals of Physics* **360**, 694 (2015).
  - [6] I. Kukuljan and T. Prosen, *Journal of Statistical Mechanics: Theory and Experiment* **2016**, 043305 (2016).
  - [7] L. D'Alessio and A. Polkovnikov, *Annals of Physics* **333**, 19 (2013).
  - [8] P. Ponte, A. Chandran, Z. Papić, and D. A. Abanin, *Annals of Physics* **353**, 196 (2015).
  - [9] A. Lazarides, A. Das, and R. Moessner, *Physical Review Letters* **115**, 030402 (2015).
  - [10] P. Ponte, Z. Papić, F. Huveneers, and D. A. Abanin, *Physical Review Letters* **114**, 140401 (2015).
  - [11] D. A. Abanin, W. De Roeck, and F. Huveneers, *Annals of Physics* **372**, 1 (2016).
  - [12] J. Rehn, A. Lazarides, F. Pollmann, and R. Moessner, *Physical Review B* **94**, 020201 (2016).
  - [13] S. Gopalakrishnan, M. Knap, and E. Demler, *Physical Review B* **94**, 094201 (2016).
  - [14] P. W. Anderson, *Physical Review* **109**, 1492 (1958).
  - [15] D. M. Basko, I. L. Aleiner, and B. L. Altshuler, *Annals of Physics* **321**, 1126 (2006).
  - [16] I. V. Gornyi, A. D. Mirlin, and D. G. Polyakov, *Physical Review Letters* **95**, 206603 (2005).
  - [17] V. Oganesyan and D. A. Huse, *Physical Review B* **75**, 155111 (2007).
  - [18] R. Nandkishore and D. A. Huse, *Annual Review of Condensed Matter Physics* **6**, 15 (2015).
  - [19] R. Moessner and S. L. Sondhi, *arXiv:1701.08056*.
  - [20] P. Titum, E. Berg, M. S. Rudner, G. Refael, and N. H. Lindner, *Physical Review X* **6**, 021013 (2016).
  - [21] V. Khemani, A. Lazarides, R. Moessner, and S. L. Sondhi, *Physical Review Letters* **116**, 250401 (2016).
  - [22] C. W. Von Keyserlingk, V. Khemani, and S. L. Sondhi, *Physical Review B* **94**, 085112 (2016).
  - [23] C. W. Von Keyserlingk and S. L. Sondhi, *Physical Review B* **93**, 245145 (2016).
  - [24] C. W. von Keyserlingk and S. L. Sondhi, *arXiv:1602.06949*.
  - [25] D. V. Else and C. Nayak, *Physical Review B* **93**, 201103 (2016).
  - [26] D. V. Else, B. Bauer, and C. Nayak, *Physical Review Letters* **117**, 090402 (2016).
  - [27] I.-D. Potirniche, A. C. Potter, M. Schleier-Smith, A. Vishwanath, and N. Y. Yao, *arXiv:1610.07611*.
  - [28] A. C. Potter, T. Morimoto, and A. Vishwanath, *Physical Review X* **6**, 041001 (2016).
  - [29] F. Nathan, M. S. Rudner, N. H. Lindner, E. Berg, and G. Refael, *arXiv:1610.03590*.
  - [30] H. C. Po, L. Fidkowski, T. Morimoto, A. C. Potter, and A. Vishwanath, *Phys. Rev. X* **6**, 041070 (2016).
  - [31] Y. Bar Lev, G. Cohen, and D. R. Reichman, *Physical Review Letters* **114**, 100601 (2015).
  - [32] S. Bera, H. Schomerus, F. Heidrich-Meisner, and J. H. Bardarson, *Physical Review Letters* **115**, 046603 (2015).
  - [33] D. H. Dunlap and V. M. Kenkre, *Physical Review B* **34**, 3625 (1986).
  - [34] F. Grossmann, T. Dittrich, P. Jung, and P. Hänggi, *Physical Review Letters* **67**, 516 (1991).
  - [35] H. Lignier, C. Sias, D. Ciampini, Y. Singh, A. Zenesini, O. Morsch, and E. Arimondo, *Physical Review Letters* **99**, 220403 (2007).
  - [36] A. Eckardt, *arXiv:1606.08041*.
  - [37] A. Eckardt, C. Weiss, and M. Holthaus, *Physical Review Letters* **95**, 260404 (2005).
  - [38] A. Zenesini, H. Lignier, D. Ciampini, O. Morsch, and E. Arimondo, *Physical Review Letters* **102**, 100403 (2009).
  - [39] M. Holthaus, G. H. Ristow, and D. W. Hone, *Physical Review Letters* **75**, 3914 (1995).
  - [40] D. W. Hone and M. Holthaus, *Physical Review B* **48**, 15123 (1993).
  - [41] D. F. Martinez and R. A. Molina, *Physical Review B* **73**, 073104 (2006).
  - [42] K. Drese and M. Holthaus, *Physical Review Letters* **78**, 2932 (1997).
  - [43] L. D'Alessio and M. Rigol, *Physical Review X* **4**, 041048 (2014).
  - [44] M. Bukov, L. D'Alessio, and A. Polkovnikov, *Advances in Physics* **64**, 139 (2015).
  - [45] A. Pal and D. A. Huse, *Physical Review B* **82**, 174411 (2010).
  - [46] R. P. Feynman, R. B. Leighton, M. Sands, and R. B. Lindsay, "The feynman lectures on physics, vol. 3: Quantum mechanics," (1966).
  - [47] A. Haldar and A. Das, *arXiv:1702.03455*.
  - [48] M. Serbyn, Z. Papić, and D. A. Abanin, *Physical Review Letters* **111**, 127201 (2013).
  - [49] D. A. Huse, R. Nandkishore, and V. Oganesyan, *Physical Review B* **90**, 174202 (2014).
  - [50] V. Ros, M. Mueller, and A. Scardicchio, *Nuclear Physics B* **900**, 420 (2014).
  - [51] A. Chandran, I. H. Kim, G. Vidal, and D. A. Abanin, *Physical Review B* **91**, 085425 (2015).
  - [52] M. Schreiber, S. S. Hodgman, P. Bordia, H. P. Lüschen, M. H. Fischer, R. Vosk, E. Altman, U. Schneider, and I. Bloch, *Science* **349**, 842 (2015).
  - [53] P. Bordia, H. Luschen, U. Schneider, M. Knap, and I. Bloch, *Nat Phys* (2017).

- [54] D. J. Luitz, N. Laflorencie, and F. Alet, Physical Review B **93**, 060201 (2016).
- [55] S. Iyer, V. Oganesyan, G. Refael, and D. A. Huse, Physical Review B **87**, 134202 (2013).
- [56] S. F. Edwards and P. W. Anderson, Journal of Physics F: Metal Physics **5**, 965 (1975).
- [57] M. Bukov, S. Gopalakrishnan, M. Knap, and E. Demler, Physical Review Letters **115**, 205301 (2015).
- [58] A. L. Burin, arXiv:1702.01431.